Journal of Solid State Chemistry **166,** 245–250 (2002)
doi:10.1006/jssc.2002.9597, available online at http://www.idealibrary.com on IDEAL®

Crystal Growth and Structure Determination of $LaMIn_5$ (M = Co, Rh, Ir)

Robin T. Macaluso,* J. L. Sarrao,† P. G. Pagliuso,† N. O. Moreno,† R. G. Goodrich,‡ D. A. Browne,‡ Frank R. Fronczek,* and Julia Y. Chan*,[1]

*Department of Chemistry, Louisiana State University, 232 Choppin Hall, Baton Rouge, Louisiana 70803; †Condensed Matter and Thermal Physics, Los Alamos National Laboratory, Los Alamos, New Mexico 87545; ‡Department of Physics and Astronomy, Louisiana State University, Baton Rouge, Louisiana 70803

Received December 26, 2001; received in revised form March 11, 2002; accepted March 22, 2002

The compounds $CeMIn_5$ (M= Co, Rh, Ir) have been shown to exhibit heavy fermion behavior. In order to better understand this effect and the nature of the observed superconductivity, we have synthesized and characterized the non-magnetic analogs, $LaMIn_5$ (M= Co, Rh, Ir). The structures of $LaCoIn_5$, $LaRhIn_5$, and $LaIrIn_5$ were determined by single-crystal X-ray diffraction. $CeMIn_5$ and $LaMIn_5$ compounds are isostructural and adopt a tetragonal structure with space group $P4/mmm$, $Z = 1$. Lattice parameters are $a = 4.6399(4)$ and $c = 7.6151(6)$ Å for $LaCoIn_5$, $a = 4.6768(3)$ and $c = 7.5988(7)$ Å for $LaRhIn_5$, and $a = 4.6897(6)$ and $c = 7.5788(12)$ Å for $LaIrIn_5$. We compare these experimental data with band structure computations and examine structural trends that affect the magnetic and transport properties of these compounds. © 2002 Elsevier Science (USA)

Key Words: **heavy fermion; single-crystal; rare-earth intermetallics; superconductivity; $LaCoIn_5$; $LaRhIn_5$; $LaIrIn_5$.**

INTRODUCTION

It is well known that BCS superconductivity is a result of electron–phonon interaction, whereas the heavy fermion superconductivity involves strong f-electron-conduction electron interactions (1). At room temperature, heavy fermion materials behave as normal metals where the f-electrons interact weakly with conduction electrons and display local-moment magnetic properties, but at low temperatures ($T \leq 20$ K), the unique and interesting properties of heavy fermion materials are manifested. The strong coupling between conduction electrons and f-electrons results in an enhanced linear-in-T contribution to the specific heat (with γ typically greater than 400 mJ/mol K^2). This corresponds to the conduction electrons having an effective mass that is typically 100 times that of a free electron, hence the term, "heavy fermion (2)."

A few heavy fermion materials become superconducting. In UBe_{13} (3), URu_2Si_2 (4, 5), UPt_3 (6), UNi_2Al_3 (7), and UPd_2Al_3 (8, 9), there are antiferromagnetic transitions followed by superconducting transitions ranging between 0.5 and 4.6 K. Four Ce compounds are also superconductors — $CeCu_2Si_2$ (10) and the more recently discovered, $CeMIn_5$ (M = Co, Rh, Ir) (11–13). Although the ordering temperatures are below 2.5 K in these heavy fermion compounds, magnetism and superconductivity can coexist.

$CeRhIn_5$ is antiferromagnetic at ambient pressure ($T_N = 3.8$ K) and superconducting at pressures above 16 kbar (14). Recently, a Fermi surface (FS) determination of a continuous series of alloys of $La_{1-x}Ce_xRhIn_5$ showed conclusively that the Ce $4f$ electrons are localized and that the band structure of $CeRhIn_5$ is best represented by the band structure of $LaRhIn_5$, rather than a delocalized $4f$ Ce band structure (15). $CeIrIn_5$ is an ambient pressure superconductor at 0.4 K (14). There is preliminary dHvA evidence that the Ce $4f$ electrons in superconducting $CeIrIn_5$ and $CeCoIn_5$ are much more strongly interacting with the conduction electrons leading to a delocalized $4f$ electron picture for the band structure in these cases (16). Of the three $CeMIn_5$ (M= Co, Rh, Ir) compounds, $CeCoIn_5$ has the highest T_c (2.3 K) (12). Superconductivity in two dimensions is thought to be common in the copper-oxide-based high T_c materials, and the upper critical field of $CeCoIn_5$ below 0.5 K is found to be highly anisotropic.

In order to understand the unusual physical properties of these layered Ce-based materials, it is important to understand the properties of the same material without the presence of the $4f$ electrons, be they localized or itinerant. For this reason, we have performed detailed studies of the structures of $LaMIn_5$ (M= Co, Rh, Ir) and made comparisons to the Ce-based structures.

[1]To whom correspondence should be addressed. Fax: +1-225-578-3458. E-mail: julia.chan@chem.lsu.edu.

0022-4596/02 $35.00

SYNTHESIS

La metal (99.999%) obtained from Ames Laboratory and In metal (Alfa Aesar, 99.9995%) were cut into small pieces. Co (Alfa Aesar, 99.998%), Rh (Alfa Aesar, 99.995%), and Ir (Alfa Aesar, 99.95%) powders were used as received. The LaMIn$_5$ compounds were prepared by measuring the constituents in a 1:1:20 ratio and placing them in an alumina crucible. Quartz wool was placed over the reaction crucible, and the entire reaction was sealed in an evacuated quartz tube. For M= Rh, Ir, the mixtures were then heated to 1100°C for 2 h and then slowly cooled to 700°C at a rate of 10°C/h. The cobalt samples were heated to 1150°C for 2 h followed by an initial rapid cooling (150°C/h) to 800°C and a slow cooling (4°C/h) to 350°C. The tube and its contents were then centrifuged to filter the excess In flux. The large $1 \times 2\,\text{mm}^2$ metallic plate-like crystals were mechanically separated for structural analysis. All of the crystals were stable in air, and no noticeable degradation of the sample was observed in magnetic measurements.

SINGLE-CRYSTAL X-RAY DIFFRACTION

A single-crystal fragment of each compound ($0.075 \times 0.025 \times 0.025\,\text{mm}^3$, LaCoIn$_5$), ($0.075 \times 0.050 \times 0.012\,\text{mm}^3$, LaRhIn$_5$), ($0.10 \times 0.08 \times 0.06\,\text{mm}^3$, LaIrIn$_5$) was mounted on a Nonius KappaCCD diffractometer (Mo$K\alpha$, $\lambda = 0.71073$ Å). Data were collected at 298 K. Further data collection parameters and crystallographic data are presented in Table 1.

The structures were refined using SHELXL97 (17) beginning with the atomic positions of the corresponding isostructural analogues, CeMIn$_5$ (M= Co, Rh, Ir) as the initial structural model (18, 19). Data were corrected for extinction and refined with anisotropic displacement parameters. The atomic coordinates are provided in Table 2, and relevant interatomic distances are given in Table 3.

CALCULATIONS

Optimal lattice parameters and atomic positions were computed using a full potential LAPW band structure code (20) employing the GGA exchange potential (21) . The

TABLE 1
Crystallographic Parameters

Formula	LaCoIn$_5$	LaRhIn$_5$	LaIrIn$_5$
Crystal data			
a (Å)	4.6399(4)	4.6768(3)	4.6897(6)
c (Å)	7.6151(6)	7.5988(7)	7.5788(12)
V (Å^3)	163.94(2)	166.20(2)	166.68(4)
Z	1	1	1
Crystal dimension (mm)	$0.075 \times 0.025 \times 0.025$	$0.075 \times 0.050 \times 0.012$	$0.10 \times 0.08 \times 0.06$
Crystal system	Tetragonal	Tetragonal	Tetragonal
Space group	*P*4/*mmm*	*P*4/*mmm*	*P*4/*mmm*
θ range(°)	2.5–35.0	2.5–35.0	2.5–32.0
μ (mm^{-1})	25.96	25.59	42.99
Data collection			
Measured reflections	1404	2000	1312
Independent reflections	263	266	203
Reflections with $I > 2\sigma(I)$	239	248	194
R_{int}	0.082	0.047	0.077
h	$-7 \rightarrow 7$	$-7 \rightarrow 7$	$-6 \rightarrow 6$
k	$-5 \rightarrow 5$	$-5 \rightarrow 5$	$-4 \rightarrow 4$
l	$-8 \rightarrow 12$	$-11 \rightarrow 12$	$-10 \rightarrow 11$
Refinement			
$R[F^2 > 2\sigma(F^2)]$	0.036	0.023	0.036
w$R(F^2)$	0.103	0.053	0.083
Reflections	263	266	203
Parameters	12	12	11
$\Delta\rho_{\text{max}}$ (e Å^{-3})	3.24	4.37	4.52
$\Delta\rho_{\text{min}}$ (e Å^{-3})	−2.06	−1.64	−3.70
Extinction coefficient	0.042(4)	0.0066(8)	None

TABLE 2
Atomic Positions and Lattice Parameters of LnMIn$_5$ (Ln = La, Ce; M = Co, Rh, Ir) (Data for the Ce Analogs Were Obtained from Refs (18) and (19))

Atom		x	y	z
Ln	1a	0	0	0
M	1b	0	0	1/2
In1	1c	1/2	1/2	0
In2	4i	0	1/2	zIn2

Experimental Compound	a (Å)	c (Å)	zIn2
CeCoIn$_5$	4.61292(9)	7.5513(2)	0.3094(3)
CeRhIn$_5$	4.656(2)	7.542(1)	0.3059(2)
CeIrIn$_5$	4.674(1)	7.501(5)	0.30524(18)
LaCoIn$_5$	4.6399(4)	7.6151(6)	0.31134(9)
LaRhIn5	4.6768(3)	7.5988(7)	0.30775(6)
LaIrIn$_5$	4.6897(6)	7.5788(12)	0.30766(16)

Computed Compound	a (Å)	c (Å)	zIn2	V/V_{exp}[a]
LaCoIn$_5$	4.675(1)	7.682(8)	0.3118(1)	1.024
LaRhIn$_5$	4.744(1)	7.702(3)	0.3067(6)	1.043
LaIrIn$_5$	4.77(2)	7.67(1)	0.305(6)	1.042

[a] V/V_{exp}= Ratio of computed cell volume to experimental cell volume of LaMIn$_5$ (M= Co, Rh, Ir).

TABLE 3
Select Interatomic Distances (Å) and Angles for LaMIn$_5$ (M = Co, Rh, Ir)

	LaCoIn$_5$	LaRhIn$_5$	LaIrIn$_5$
Within cuboctahedron			
In1–In2	3.3171(5)	3.3071(4)	3.3068(9)
La–In1 (× 4) (Å)	3.2809(3)	3.3070(2)	3.3161(4)
La–In2 (× 8) (Å)	3.3171(5)	3.3071(4)	3.3068(9)
	Angles (deg)	Angles (deg)	Angles (deg)
In1–La–In1	90	90	90
In1–La–In2	119.640 (5)	119.999 (3)	120.093 (9)
In1-La-In2	60.360 (5)	60.001 (3)	59.907 (9)
In2-La-In2	59.279 (10)	59.999 (8)	60.186 (19)
In2-La-In2	88.755 (18)	89.998 (13)	89.68 (3)
In2-La-In2	120.721 (10)	119.999 (3)	119.813
Within rectangular polyhedron			
In2–In2 (c-axis)	2.8733(14)	2.9218(9)	2.915(2)
In2–In2 (a–b plane)	3.2809(3)	3.3070(2)	3.3161(4)
M–In2 (× 8) (Å)	2.7288(4)	2.7572(3)	2.7610(7)
	Angles (deg)	Angles (deg)	Angles (deg)
In2–M–In2	63.54(3)	63.990(17)	63.74(4)
In2–M–In2	73.907(12)	73.696(8)	73.81(2)

muffin–tin radii were 2.85 a.u. for La, 2.50 a.u. for In, 2.55 a.u. for Co and Rh, and 2.6 a.u. for Ir. A total of 690 plane waves, corresponding to an energy cutoff of 30 Ry, were used. The Brillouin zone integrations were done over 330 kpts in the irreducible wedge (5000 points in the full zone). The core levels were treated completely relativistically, while the spin–orbit interaction in the valence states was included as a perturbation. The total energy was minimized to 30 μRy by varying a, c, and the z position of the In2 site. The residual forces in the converged structure were smaller than 3 mRy/a.u.

RESULTS AND DISCUSSION

LaMIn$_5$ (M= Co, Rh, Ir) are found to be isostructural to their Ce analogs with the HoCoGa$_5$ structure type in the tetragonal space group $P4/mmm$ (22). The structure is shown in Fig. 1 and consists of four atoms in the asymmetric unit where La, M, In1, and In2 atoms occupy the 1a, 1b, 1c, and 4i sites, respectively.

Like high-temperature superconducting cuprates, LnMIn$_5$ (Ln= La, Ce; M = Co, Rh, Ir) can be described as a layered compound. In CeCoIn$_5$, for example, critical-field measurements in the a–c plane have suggested two-dimensional superconductivity (23). In LaMIn$_5$, the multilayers are seen as 8-coordinated CoIn$_2$ rectangular prisms interleaved with face-sharing layers of LaIn$_3$ cuboctahedra. For LaCoIn$_5$, the height of the LaIn$_3$ cuboctahedra layer and the CoIn$_2$ layers are 4.742 and 2.873 Å, respectively.

The layered structure can also be viewed as alternating La–In planes and M–In planes. These sheets are stacked directly above one another; the transition metal atoms lie directly above the lanthanide atoms (La or Ce), and the planar Ln–Ln distances are equivalent to the planar M–M distances. For M= Co, Rh, Ir, respectively, these intraplanar La–La and M–M distances are 4.6399(4), 4.6768(3), and 4.6897(6) Å.

The coordination of the La in the cuboctahedra is 12-fold to In: fourfold to In1 and eightfold to In2. The La–In2 coordination of the cuboctahedra includes eight equivalent La–In2 bond distances of 3.2809(3), 3.3070(2), and 3.3161(4) Å for M= Co, Rh, Ir, respectively. This is in good agreement with other La–In distances in the binary compounds: InLa (24), InLa$_3$, In$_2$La (25), and In$_3$La (25,26), where La–In2 distances range from 3.226 to 3.596 Å.

The Ce–In and La–In bond distances are shown in Table 4. In the CeMIn$_5$ analogs, the ratio between Ce–In2 and Ce–In1 distances showed that the cuboctahedra of CeCoIn$_5$ were distorted in such a manner that the c-axis was elongated (18). The cuboctahedra of CeIrIn$_5$, on the other hand, were shortened along the c-axis. In CeRhIn$_5$,

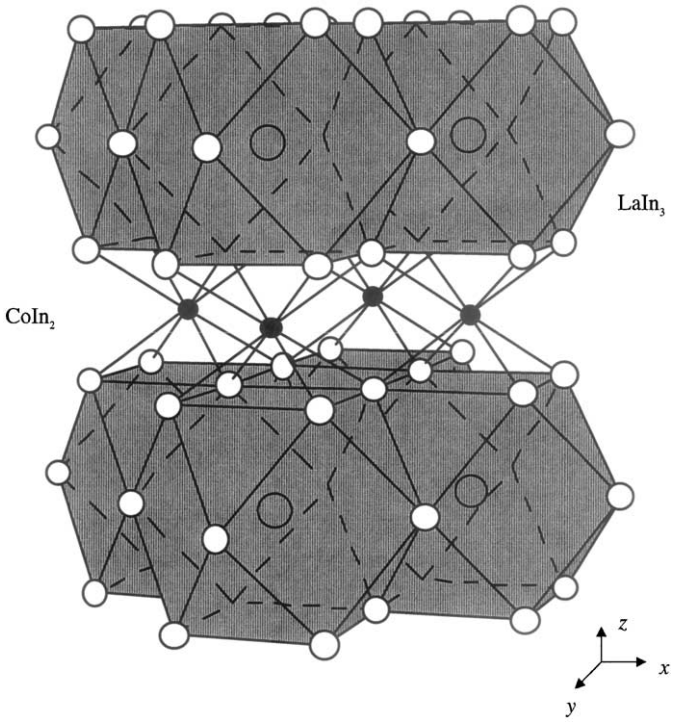

FIG. 1. Layers of $LaIn_3$ cuboctahedra and $CoIn_2$ rectangular prisms alternate along the *c*-axis. La are coordinated to eight In1 and four In2 atoms. The body-centered La is represented by the gray shading of the prism; Co is represented by the black circles, and In is represented by the white circles.

the Ce–In2: Ce–In1 ratio is very close to one, indicating that the cuboctahedron is under minimal distortion.

The trend is similar in the LaMIn$_5$ series. The ratio of La–In2 and La–In1 distances reveals a distorted cuboctahedron in $LaCoIn_5$ and $LaIrIn_5$, whereas all La–In distances in the $LaRhIn_5$ cuboctahedra are identical to each other. The cuboctahedra, which are formed from La and In1 and In2 atoms are neither distorted along the *c*-axis nor the *a*–*b* plane. The La–In1 and La–In2 distances, 3.3070(2) and 3.3071(4) Å, are identical. For $LaCoIn_5$, the La–In1 interatomic distances, 3.2809(3) Å, are shorter than the La–In2 distances of 3.3171(5) Å, thus indicating an elongated *c*-axis. The *c*-axis of $LaIrIn_5$ is shortened with La–In1 distances of 3.3162(4) Å while the La–In2 bond distance within the cuboctahedra is only 3.3068(9) Å.

The transition metal is coordinated to eight In2 atoms forming a rectangular prism.. Each pair of In2 atoms along the *c*-axis forms the edge of a neighboring rectangular prism. The *M*–In distances are 2.7288(4), 2.7572(3), 2.7610(7) Å for $LaCoIn_5$, $LaRhIn_5$, and $LaIrIn_5$, respectively. These values are in good agreement with $CoIn_2$ (27) $CoIn_3$ (28, 29), InRh (30), and $IrIn_3$ (31), where Co–In distances range from 2.601 to 2.763 Å.The transition metal in the binary alloys, $CoIn_3$ (28), InRh (30), and $IrIn_3$ (31), and in the heavy fermion compounds all have a coordination number of eight. The In–In interatomic distances are also similar to $CoIn_2$ and $CoIn_3$ with In-In distances in the range of 3.135–3.596 Å. For $LaCoIn_5$, In–In distances are 3.2809(3) (*a*–*b* plane) and 2.8733(14) Å (*c*-axis).

Trends in the lattice parameters are similar to those previously reported for the CeMIn$_5$ (M= Co, Rh, Ir) analogs (M= Co, Rh, Ir), with the La values being slightly larger due to expected lanthanide contraction (18). It was found that the *a*-axis becomes elongated and the *c*-axis becomes shortened as the atomic radius of the transition metal increases. As provided in Table 4, the cuboctahedra *c*-axis (La–In2 interatomic distance) and the In2–La–In2 angle decrease as the transition metal becomes larger. This accompanies the increase in the *M*–In bond and the In2–In2 bond distances of the rectangular prisms along the plane and the *c*-axis. The expansion of the *c*-axis in the rectangular prisms is not sufficient to compensate for the decrease in the height of the cuboctahedra.

The atomic positions for the 4*i* sites are shown in Table 2. Similar to the CeMIn$_5$ analogs, the position is further away from the transition metal as the atomic size increases from Co to Ir. This trend in the *z* position of In2 is due to the expansion of the rectangular prisms along the *c*-axis.

The Rh compounds show similar structural features in the $LnIn_3$ cuboctahedra in both the CeMIn$_5$ and LaMIn$_5$ analogues. $LaIn_3$ is known to be a cubic (25, 26) and in $LaRhIn_5$, all the *a* and *c* axes of the $LaIn_3$ layers are equivalent to 4.6768(3) Å. The cubic structure is reflected in the La–In2:La–In1 ratio, and it is only when this ratio is close to unity that a small piece of Fermi surface is observed at 7 T (32).

The computed optimal lattice structure agrees with the experimental data. Results from the computations are summarized in Table 2. General trends in variations of the lattice parameters and atomic positions are reproduced in the calculations, although the calculated *a* and *c* parameters are somewhat larger than the experimental values.

TABLE 4
Ln–In Bond Distances in Cuboctahedra for *Ln* = La, Ce (Data for the Ce Analogs Were Obtained from Refs (18) and (19))

	Ce–In2 (Å)	Ce–In1 (Å)	Ce–In2/Ce-In1
Co	3.283(1)	3.26183(6)	1.006
Rh	3.2775(7)	3.292(2)	0.9956
Ir	3.272(1)	3.3050(7)	0.9900
	La–In2(Å)	La–In1(Å)	La–In2/La–In1
Co	3.3171(5)	3.2809(3)	1.0110
Rh	3.3071(4)	3.3070(2)	1.000
Ir	3.3068(9)	3.3161(4)	0.99720

The agreement is closest in $LaCoIn_5$ where the difference is 0.8%, while the differences are 1.4% larger for the $LaRhIn_5$ and $LaIrIn_5$ cases.

The computed structure is not just an expanded version of the experimental one since the zIn2 values are different. Furthermore, the calculations reproduce the experimental feature that the La–In1 distance is 1% less than the La–In2 distance in $LaCoIn_5$, the distances are equal in $LaRhIn_5$ and the La–In1 distance is larger in $LaIrIn_5$.

The total energy was minimized by varying a, c, and zIn2 until the total energy was minimized to an accuracy of 30 μRy, and the minimization of the a and c lattice parameters was done by steepest descent. The minimization of zIn2 was done by two methods. In one method it was included in the steepest descent minimization, while in the other, c and a were minimized and then damped molecular dynamics was done using the calculated forces on the In atom. Both methods agree to within the precision stated, and the forces on the In2 atom at the final positions were less than 4 mRy/au. The uncertainties quoted were derived by finding how much variation in c, a, and zIn2 resulted in a rise of 30 μRy in the total energy above the minimum value. When minimizing the force on the atom, the computed uncertainty in zIn2 was consistent with the experimental value of zIn2. The fact that the calculated equilibrium lattice constants are 0.5–1.5% larger than the experimental is consistent with the typical accuracy of 1–3% that is expected for an all-electron density functional calculation of the lattice parameters.

In summary, comparisons of the structural trends of LaMIn$_5$ (M = Co, Rh, Ir) follow our expectations. The larger metal cation causes the unit cell to increase along the plane; however, in the Rh case, the lengths of the a and c axes are very similar to that of the cubic parent compound, $LaIn_3$. The calculations of the total energy have been presented to show that we are able to properly model the experimental results obtained. These calculations will be compared with Fermi surface studies and other probes of the band structure in a subsequent publication.

ACKNOWLEDGMENTS

Work at Los Alamos National Laboratory performed under the auspices of the US Department of Energy. The purchase of the single-crystal X-ray diffractometer was made possible by Grant No. LEQSF (1999–2000)-ESH-TR-13, administered by the Louisiana Board of Regents. R. T. M. and J. Y. Chan also acknowledge Grant No. LEQSF (2001–04)-RD-A-05.

REFERENCES

1. M. Tinkam, "Introduction to Superconductivity." McGraw-Hill, New York, 1996.
2. Z. Fisk, H. R. Ott, T.M. Rice, and J. L. Smith, *Science* **320,** 124 (1986).
3. H. R. Ott, H. Rudigier, Z. Fisk, and J. L. Smith, *Phys. Rev. Lett.* **50,** 1595 (1983).
4. T. T. M. Palstra, A. A. Menovsky, J. v. d. Berg, A. J. Dirkmaat, P. H. Kes, G. J. Nieuwenhuys, and J. A. Mydosh, *Phys. Rev. Lett.* **55,** 2727 (1985).
5. M. B. Maple, J. W. Chen, Y. Dalichaouch, T. Kahora, C. Rossel, M. S. Torikachvili, M. W. McElfresh, and J. D. Thompson, *Phys. Rev. Lett.* **56,** 185 (1986).
6. G. R. Stewart, Z. Fisk, J. O. Willis, and J. L. Smith, *Phys. Rev. B* **127,** 448 (1984).
7. C. Geibel, S. Thies, D. Kaczorowski, A. Mehner, A. Grauel, B. Seidel, U. Ahlheim, R. Helfrich, K. Petersen, C. D. Bredl, and F. Steglich, *Z. Phys. B Condens. Matter* **83,** 305 (1991).
8. C. Geibel, C. Schank, S. Thies, H. Kitazawa, C. D.Bredl, A. Bohm, M. Rau, A. Grauel, R. Caspary, R. Helfrich, U. Ahlheim, G. Weber, and F. Steglich, *Z. Phys. B Condens. Matter* **84,** 1 (1991).
9. C. Geibel, U. Ahlheim, C. Bredl, J. Diehl, A. Grauel, R. Helfrich, H. Kitzawa, R. Kohler, R. Modler, M. Lang, C. Schank, S. Thies, F. Steglich, N. Sato, and T. Komatsubara, *Physica C* **185,** 2651 (1991).
10. F. Steglich, J. Aarts, C. D. Bredl, W. Lieke, D. Meschede, W. Franz, and H. Schafer, *Phys. Rev. Lett.* **43,** 1892 (1979).
11. Y. M. Kalychak, V. I. Zaremba, V. M. Baranyak, V. A. Bruskov, and P. Y. Zavalii, *Izv. Akad. Nauk SSSR, Met.* **1,** 209 (1989).
12. C. Petrovic, P. G. Pagliuso, M. F. Hundley, R. Movschovich, J. L. Sarrao, J. D. Thompson, Z. Fisk, and P. Monthoux, *J. Phys. Condens. Matter* **13,** L337 (2001).
13. C. Petrovic, R. Movshovich, M. Jaime, P. G. Pagliuso, M. F. Hundley, J. L. Sarrao, Z. Fisk, and J. D. Thompson, *Europhys. Lett.* **53,** 354 (2001).
14. H. Hegger, E. G. Moshopoulou, M. F. Hundley, J. L. Sarrao, Z. Fisk, and J. D. Thompson, *Phys. Rev. Lett.* **84,** 4986 (2000).
15. U. Alver, R. G. Goodrich, N. Harrison, D. W. Hall, E. C. Palm, T. P. Murphy, S. W. Tozer, P. G. Pagliuso, N. O. Moreno, J. L. Sarrao, and Z. Fisk, *Phys. Rev. B* **64,** 180402 (2001).
16. R. G. Goodrich, U. Alver, N. Harrison, J. L. Sarrao, R. T. Macaluso, and J. Y. Chan, in preparation.
17. G. M. Sheldrick, "SHELXL97," University of Gottingen, Germany, 1997.
18. E. G. Moshopoulou, Z. Fisk, J. L. Sarrao, and J. D. Thompson, *J. Solid State Chem.* **158,** 25 (2001).
19. E. G. Moshopoulou, J. L. Sarrao, P. G. Pagliuso, N. O. Moreno, J. D. Thompson, Z. Fisk, and R. M. Ibberson, *App. Phys. A: Mater. Sci. Process.*, to appear (2001).
20. P. Blaha, K. Schwarz, and J. Luitz, "A Full Potential Linearized Augmented Plane Wave Package for Calculating Crystal Properties, WIEN97." Karlheinz Schwarz, Techn. Universitat Wien, Austria, 1999.
21. J. P. Perdew, S. Burke, and M. Ernzerhof, *Phys. Rev. Lett.* **77,** 3865 (1996).
22. Y. N. Grin, Y. P. Yarmolyuk, and E. I. Gladyshevskii, *Sov. Phys. Crystallogr.* **24,** 137 (1979).
23. T. P. Murphy, D. Hall, E. C. Palm, S. W. Tozer, C. Petrovic, Z. Fisk, R. G. Goodrich, P. G. Pagliuso, J. L. Sarrao, and J. D. Thompson, *Phys. Rev. B* **65,** 100514(R) (2001).
24. J. L. Moriarty, J. E. Humphreys, R. O. Gordon, and N. C. Baenziger, *Acta Crystallogr.* **21,** 840 (1966).
25. O. D. McMasters and K. A. Gschneidner, *J. Less-Common Met.* **38,** 137 (1974).
26. K. H. J. Buschow, H. W. de Wijn, and A. M. van Diepen, *J. Chem. Phys.* **50,** 137 (1969).

27. H. H. Stadelmaier and H. K. Manaktala, *Acta Crystallogr*. **31,** 374 (1975).
28. H. H. Stadelmaier, J. D. Schobel, R. A. Jones, and C. A. Shumaker, *Acta Crystallogr*. **29,** 2926 (1973).
29. M. V. Katrich, N. N. Matyushenko, and Y. N. Titov, *Sov. Phys. Crystallogr*. **22,** 107 (1977).
30. K. Schubert, H. Breimer, W. Burkhardt, E. Gunzel, R. Haufler, H. L. Lukas, H. Vetter, J. Wegst, and M. Wilkens, *Naturwissenschaften* **44,** 229 (1957).
31. M. Ellner and S. Bhan, *J. Less-Common Met*. **79,** PP1 (1980).
32. R. G. Goodrich, D. L. Maslov, A. F. Hebard, J. L. Sarrao, D. Hall, and Z. Fisk, submitted.